

Saturation Effect and Field Correction Using Holes in Yoke

R. Yamada & J. Moeller
Fermilab, Batavia, IL - 60510

Summary

With optimized conductor geometries for 45-mm and 50-mm aperture cosine- θ dipole type magnet designs, only the sextupole term changes drastically with the higher excitation of the magnet up to 12 T. To reduce the sextupole term, a set of holes is placed in the yoke and its effect on the field distribution is calculated. It is evident that the sextupole term can easily be reduced to within $\pm 1.6 \times 10^{-4}$ units in the range of 11 to 12 T, at a reference radius of 1.0 cm. With further adjustment of the holes, the peak value of the sextupole could be reduced even more.

1. Introduction

As the excitation current increases, the field distribution in the beam bore becomes increasingly distorted due to the saturation of the yoke. Usually, the sextupole term suddenly has a positive increase when the top and bottom inner yoke surfaces reach about 2.0 T. Around the circular surface of the iron, the top and bottom regions become more saturated than the side regions. Because the saturation pattern is non-uniform around the bore, a positive sextupole component is added to the field. This trend continues with increased excitation and the sextupole term peaks when the side iron starts to saturate around 2.0 T. With further increase in yoke saturation, the sextupole term gradually decreases beyond this peak. This behavior is more prominent in designs with less space between the coil and the inner surface of the iron yoke. During this cycle of operation, the other higher harmonics remain fairly small and constant [1].

2. Application of Holes in Yoke for the Correction of Iron Saturation Effect

The use of holes in the yoke for the correction of iron saturation has been tried and used with non-superconducting magnets in the past. Its application to the RHIC magnets was reportedly a success [2,3]. The holes were also applied in our design study of the 50-mm and 45-mm bore dipoles for 11 to 12 T field [1]. In such designs, the holes are introduced near the side surfaces of the yoke so that the inner iron starts to saturate at the side surfaces earlier than in the case without the holes. By trying to make the whole iron surface saturate more uniformly with the proper distribution of holes, we can reduce the magnitude of the sextupole term. We conducted case studies with 50-mm and 45-mm bore magnet designs using ANSYS. The effects of the holes are illustrated with these cases, but the principle could be applied with any bore size.

3. Programming Procedure

The case studies were performed using the Finite Element program ANSYS [4]. Two-dimensional electromagnetic models were constructed using ROXIE-derived coil cross-sections. The inner and outer radii of the iron yoke were held at fixed values throughout each study. Magnetic field calculations were first done with a solid iron yoke for comparison to other iron configurations. Magnet excitation was simulated at several key current values for each iron configuration. For each run, the solid iron configuration was modified by introducing one or more circular holes filled with a vacuum element. A solution routine was executed with load steps of various currents. The harmonic field components were then extracted in a two-step process. The radial field component, B_r , was first extracted at 1 cm using an ANSYS path operation. This data was then processed by the harmonic analysis routine TRICOF that was extracted from the program ROXIE [5]. The resulting harmonic data was then graphed versus current and analyzed. Flux line and flux density plots were also obtained to aid our understanding of the holes' re-routing effect on flux density. By correlating changes in the shape of the sextupole vs. current curve to placement of holes in the iron, we were able to reduce the sextupole presence by strategically configuring the yoke holes.

4. Case Studies

At first, the holes were applied to the yoke of the 50-mm bore magnet design. We attempted several different configurations to find one with reasonable sextupole reduction. We then applied this same hole configuration to the 45-mm bore magnet designs and observed a significant reduction in the saturation-induced sextupole. We think that the data for the 45-mm bore magnets can be improved more with further adjustment of the holes.

4.1 50-mm Bore Magnet

After the conductor configuration was optimized with the ROXIE program, the geometry was further studied for the iron saturation effect with the ANSYS program. The 50-mm design we used had a 25 mm wide collar. As shown in Figure 1a, the sextupole is the only component showing significant variation with the excitation current. The sextupole term starts to rise at 5 kA ($B_0 = 3.8$ T), and reaches about 7 units around 10 kA ($B_0 = 7.3$ T) and 12 kA ($B_0 = 8.57$ T).

We then applied several different hole configurations and their results are shown in Figure 2. The best configuration of the magnet with holes is shown in Figure 3, which shows the flux distribution at 18 kA, corresponding to the central field of $B_0 = 11.74$ T. The diameters of these holes are 70 mm, 30 mm, and 16 mm. The resulting harmonics distributions are shown in Figure 1b. The sextupole term peaks at only 1.7 units near 7.5 kA ($B_0 = 5.54$ T) and goes down almost linearly to -1.3 units at 18 kA ($B_0 = 11.74$ T).

4.2 45-mm Bore Magnet

The same procedures were applied to the two 45-mm bore designs: one with a thin 9 mm spacer and another with a 25 mm collar [1]. Their geometries and flux distributions

are shown in Figures 4a and 5a with the semi-optimized yoke hole configuration at 18 kA. The central field values B_0 for these two cases are 11.47 T and 11.27 T respectively. The magnetic flux density distributions inside the iron yoke are shown in Figures 4b and 5b. They clearly show how the holes are contributing to make the inner yoke surfaces saturate more uniformly. The diameters of these holes are 70 mm, 30mm, and 16 mm, the same as in the 50-mm design.

The excitation curves for the central magnetic field B_0 are shown in Figure 6. Their data are shown as “Thin Collar/Solid” for the 9 mm thin-spacer design with solid yoke and “Thick Collar/Solid” for the 25 mm thick-collared design with solid yoke. Also shown in Figure 6 are the excitation curves for these two magnets with the semi-optimized yoke hole configuration as “Thin Collar/Holes” and “Thick Collar/Holes.” The excitation curve of the thin collared magnet is affected by saturation much sooner than that of the thicker collared magnet. This variation in the saturation of the excitation curves is partly due to the difference in the width of the yoke of these magnets. The thin-spacer magnet has a yoke that is only 149.5 mm wide, while that of the thick collared magnet is 175.5 mm wide.

The harmonics distributions of these two magnets without saturation correction holes are shown in Figures 7a and 8a. Without correction holes, the sextupole terms reach up to 9.8 and 3.7 units for the thin-spacer and thick-collared magnets, respectively.

With the application of the best hole pattern for the 50-mm magnet to these 45-mm magnets, the maximum sextupole harmonics values are reduced to 1.6 for both types of magnet, as shown in Figures 7b and 8b. This value may be acceptable for accelerator operation, but with further adjustment it could be reduced further.

In Figure 9, the sextupole term b_3 of the thin-collared magnet without iron yoke holes is shown together with the magnetization curves of the inner iron surface at the top (90°) and on the median plane (0°). It shows the sextupole term starting to go up when the top surface (90°) reaches about 2 T, and it starts falling down when the side surface (0°) reaches about 2 T. This behavior is also observed in the case with iron yoke holes as well as the other magnet designs.

The bore field distributions of the thin-spacer design with and without iron yoke holes, which are taken directly from the ANSYS model, are shown in Figure 10. The field shape at 1 kA is identical, but it clearly shows the effect of the correction holes at 10 kA and 18 kA. This phenomenon clearly correlates to what we understand from the harmonics shown in Figures 7a and 7b.

References

- [1]. R. Yamada, J. Moeller, and M. Wake, "Design Study of 45-mm Bore Dipole Magnet for 11 to 12 Tesla Field." TD-99-012. March 26, 1999.
- [2]. R. Gupta et. al. "Field Quality Control Through the Production Phase of RHIC Arc Dipoles." Proceedings of 1995 PAC and International Conference on High Energy Accelerators. p. 1423.
- [3]. R. Gupta, "Improving the Design and Analysis of Superconducting Magnets for Particle Accelerators." Thesis. November 1996.
- [4]. J. Moeller, "ANSYS Procedure for 2D Field Analysis and Iron Saturation Study." TD-99-016, March 1999.
- [5]. Harm.exe, executable form of TRICOF harmonic analysis procedure. It was extracted from ROXIE fortran source by V. Kashikhin.

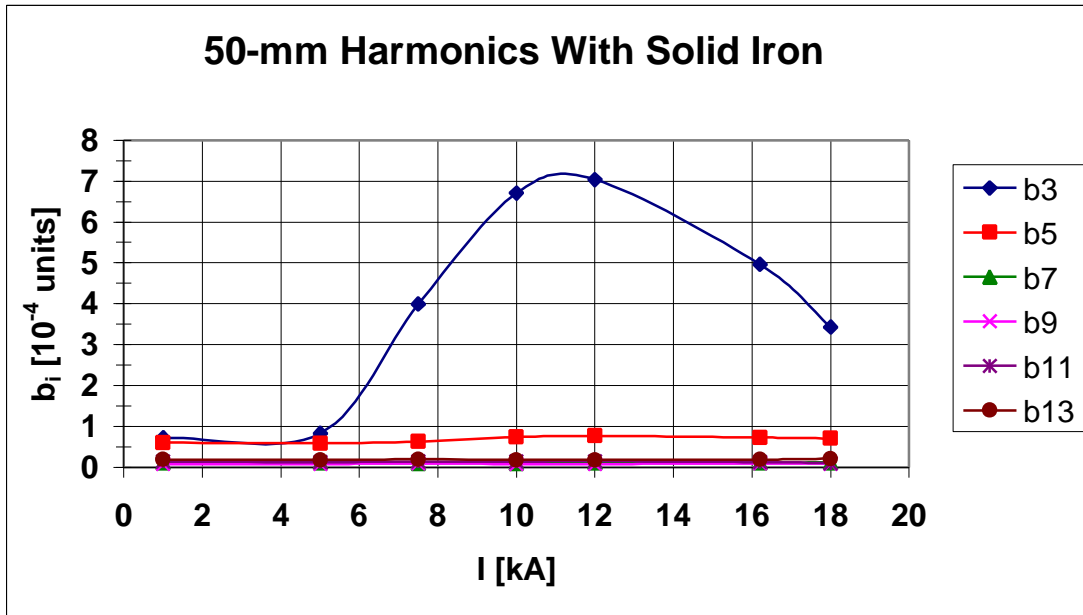


Figure 1a. Harmonics distribution for the 50-mm bore design with solid iron.

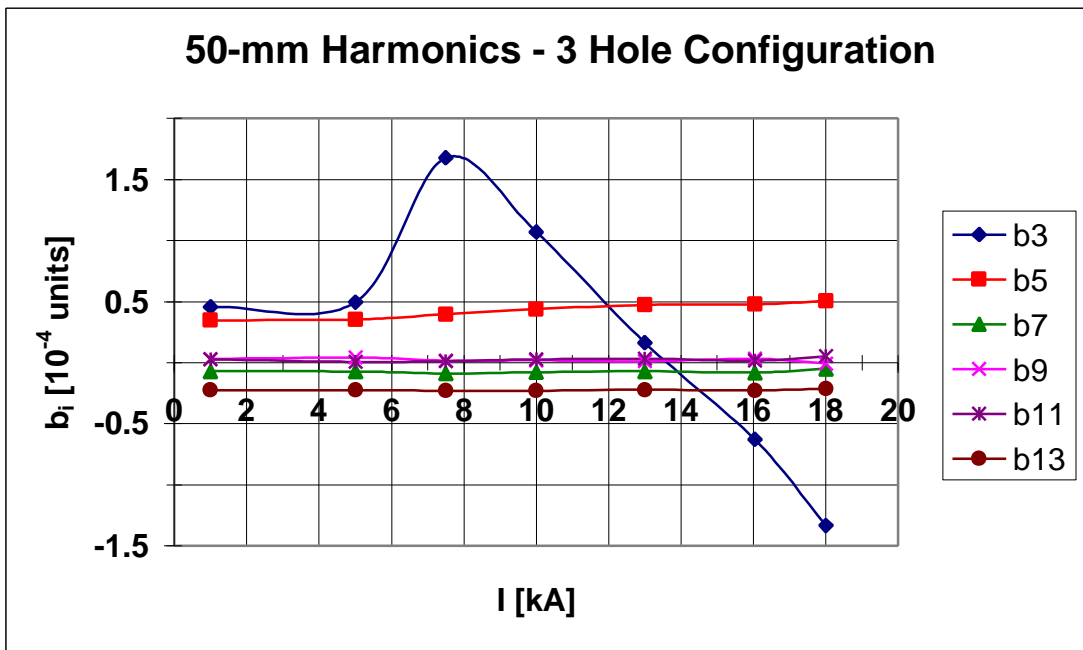


Figure 1b. Harmonics distribution for the 50-mm bore design with semi-optimized configuration of 3 holes in yoke.

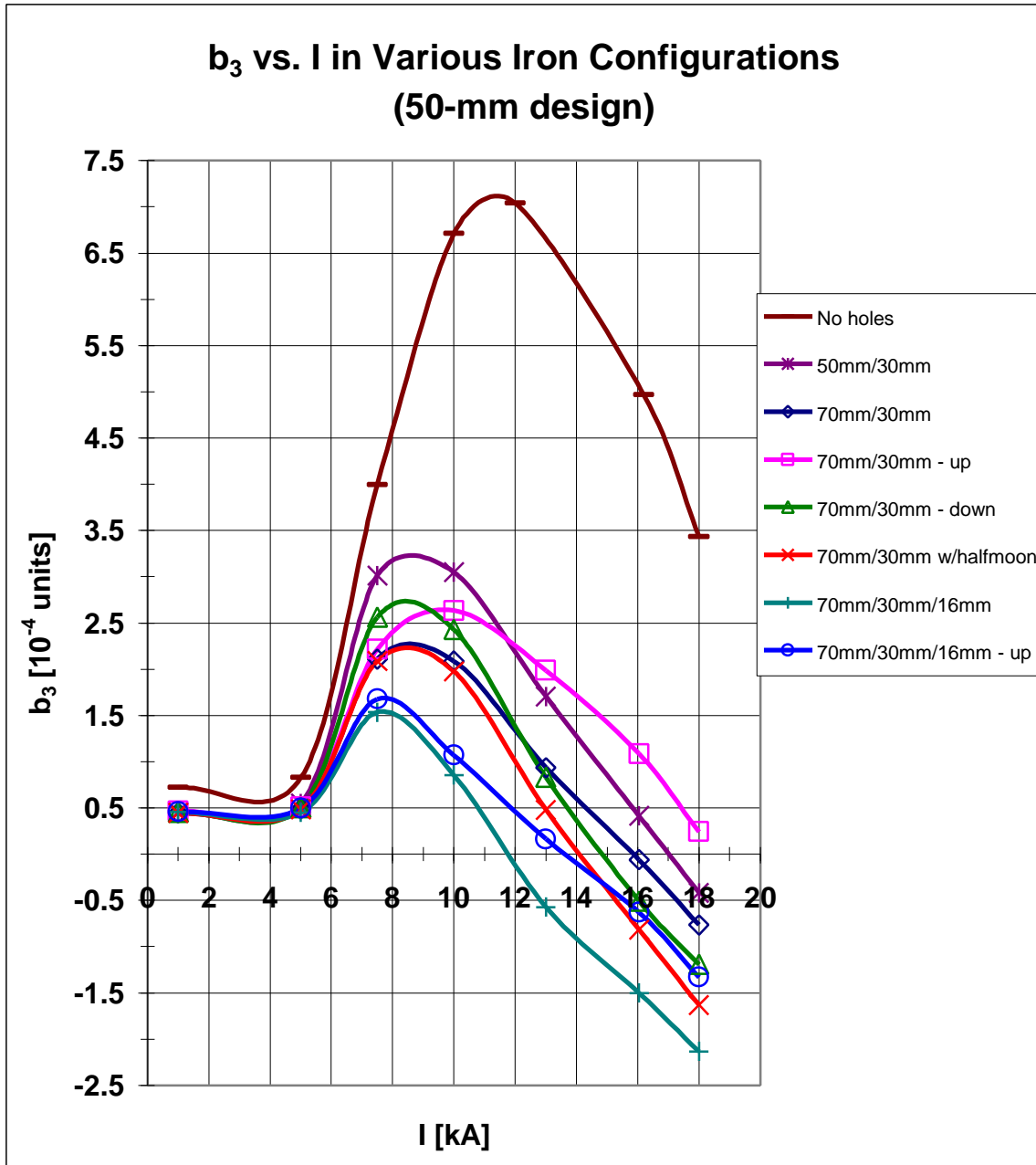


Figure 2. Comparison of sextupole variation in several iron yoke hole configurations.

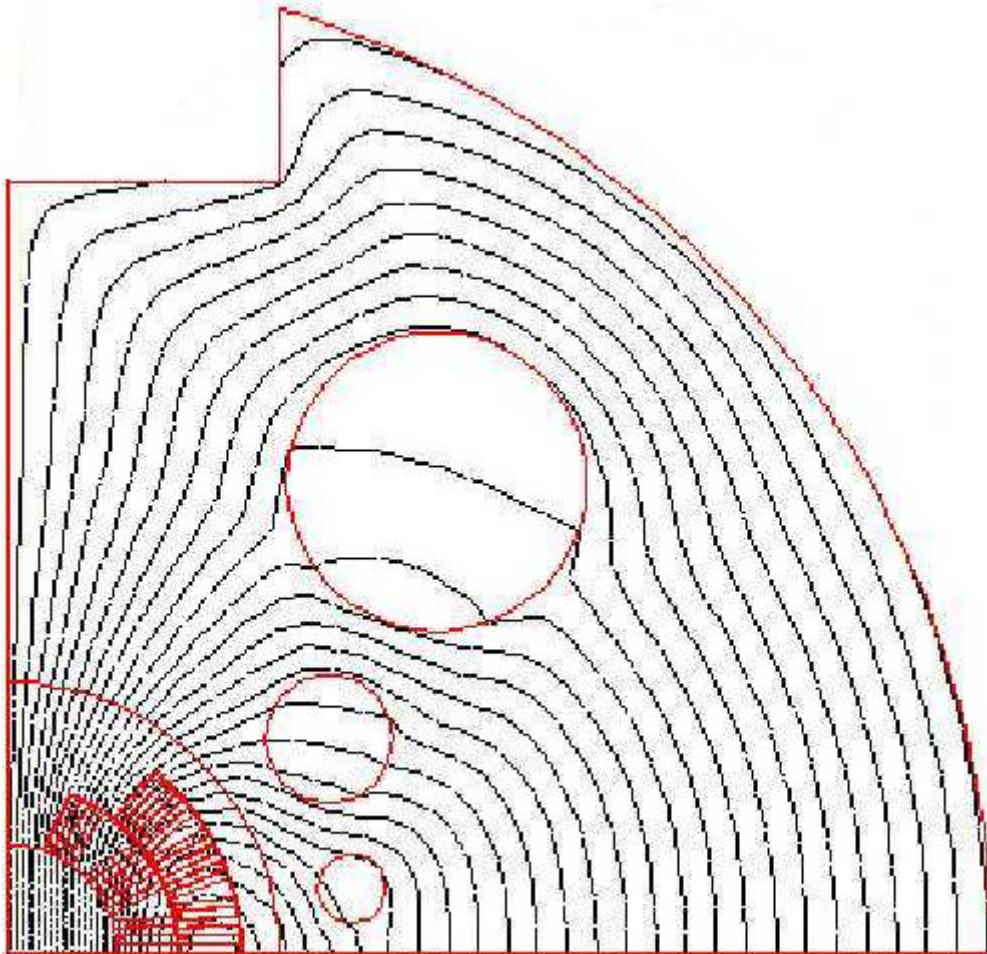


Figure 3. Geometry of the 50-mm bore design with semi-optimized yoke hole configuration and flux lines at 18 kA.

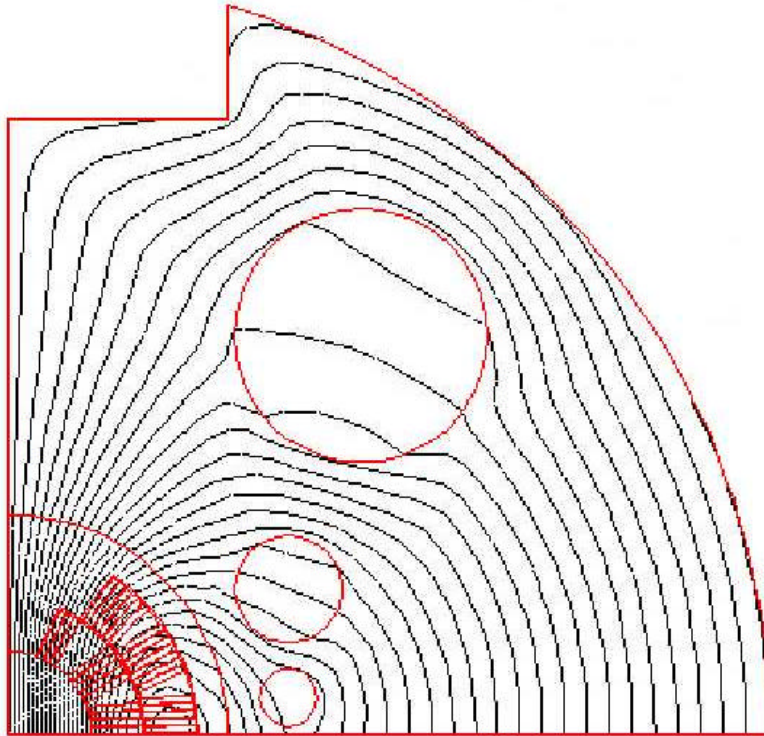


Figure 4a. Geometry of the 45-mm design with thin spacer, semi-optimized yoke hole configuration, and flux lines at 18 kA.

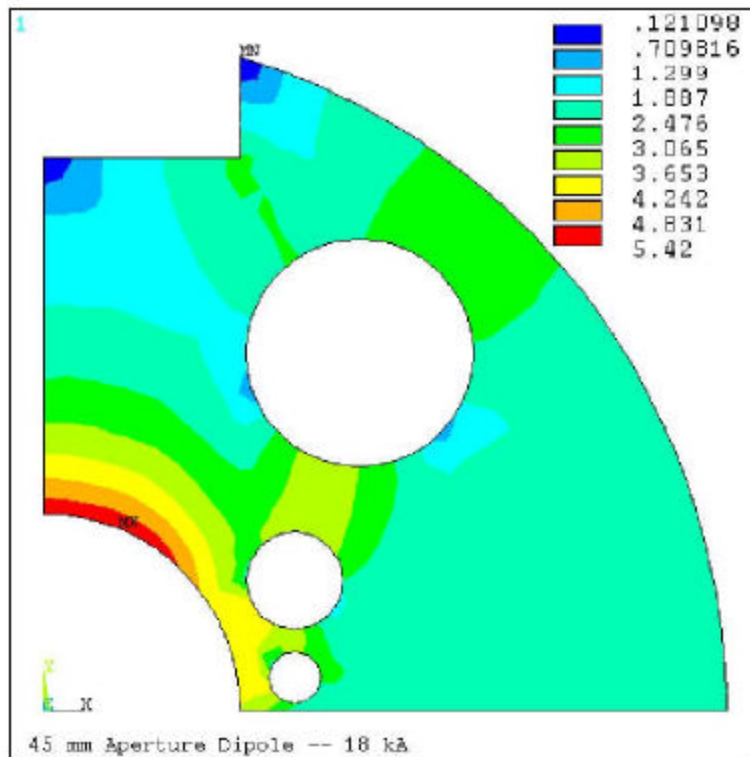


Figure 4b. Magnetic flux density inside the iron yoke for the 45-mm design with thin spacer and iron yoke holes.

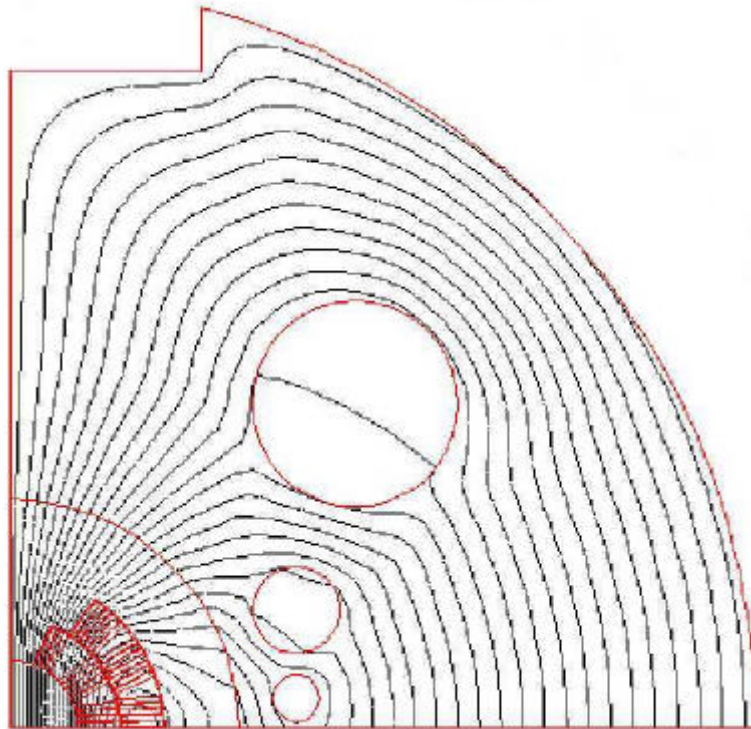


Figure 5a. Geometry of the 45-mm design with thick collar, semi-optimized yoke hole configuration, and flux lines at 18 kA.

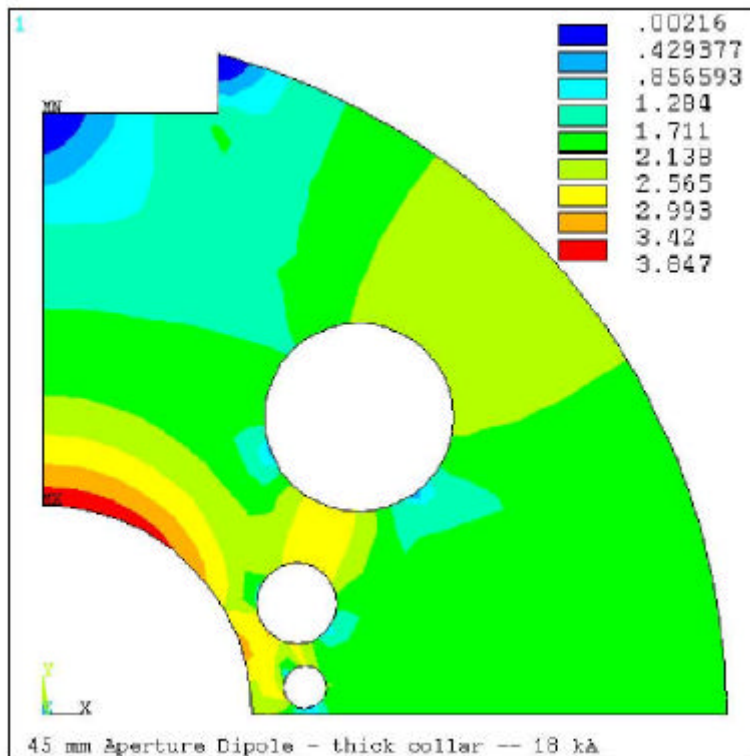


Figure 5b. Magnetic flux density inside the iron yoke for the 45-mm design with thick collar and iron yoke holes.

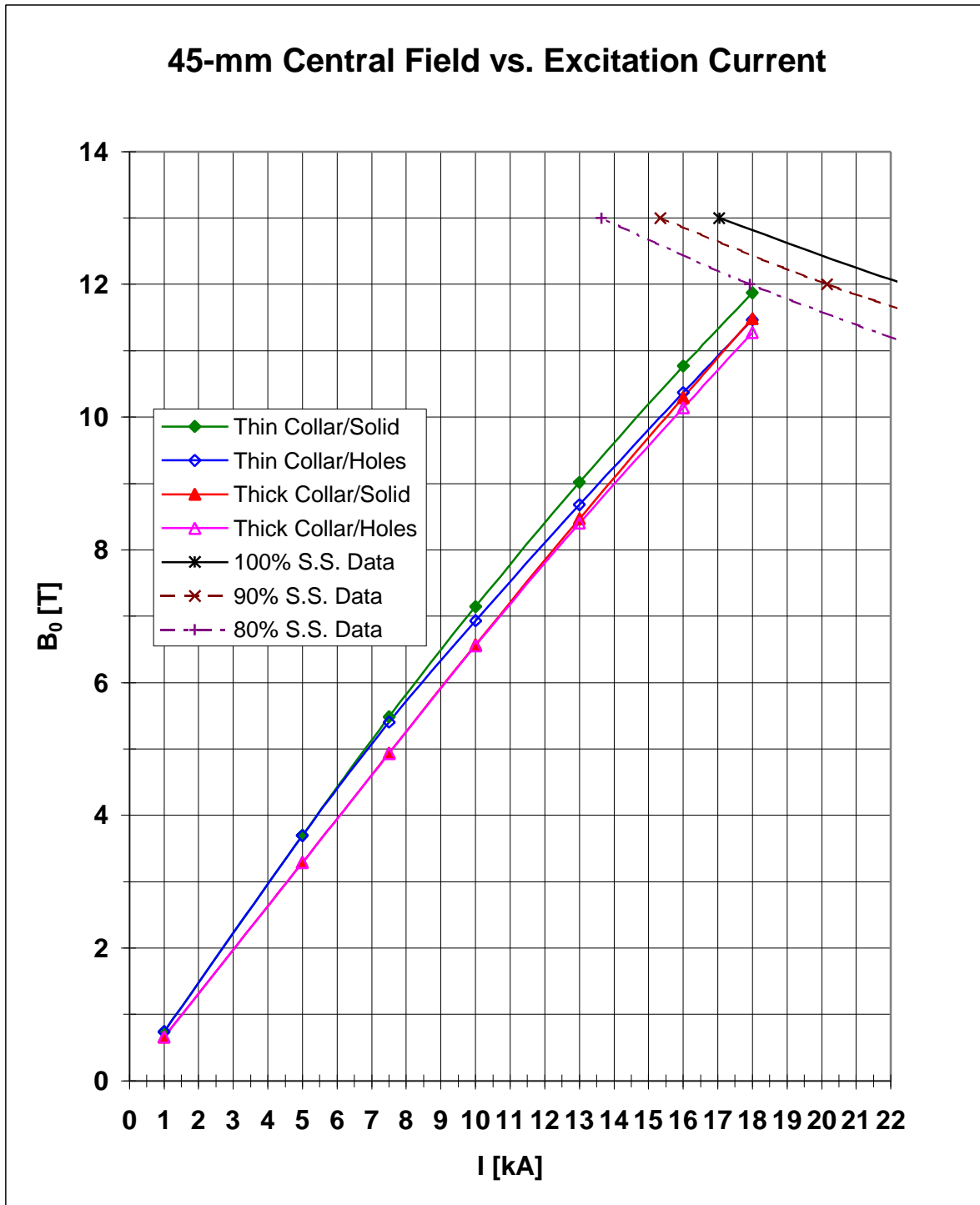


Figure 6. Excitation curves of the 45-mm bore designs with and without iron yoke holes.

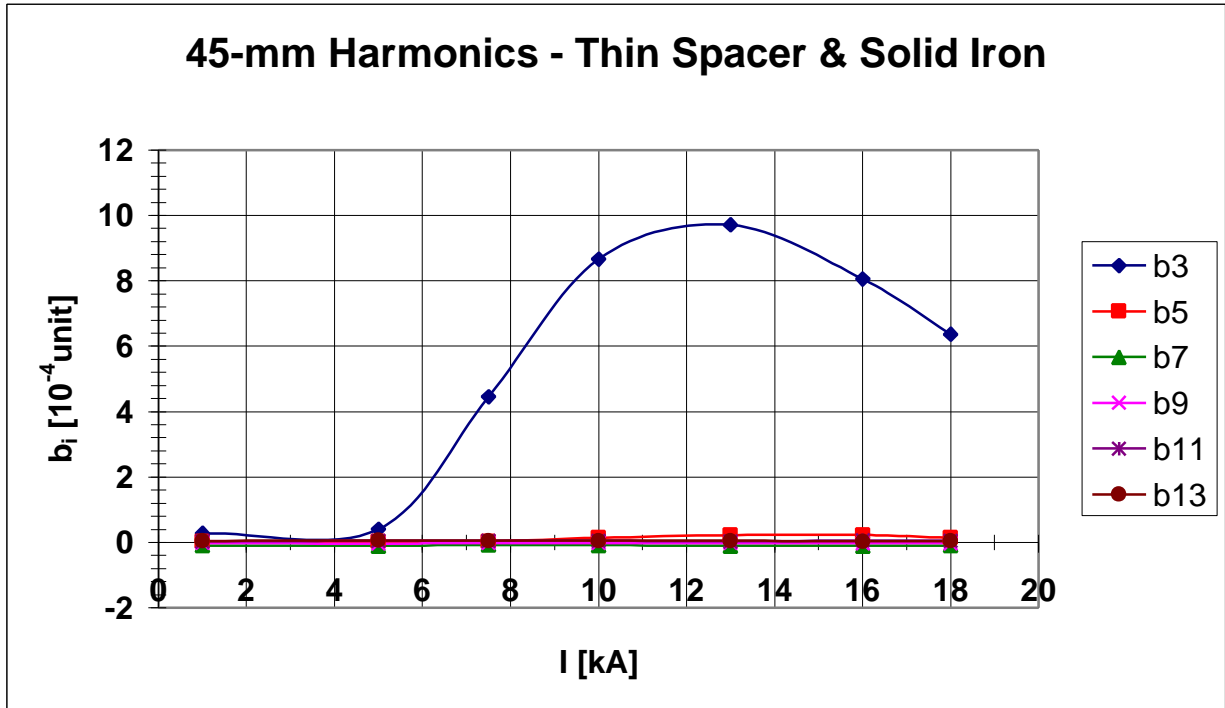


Figure 7a. Harmonics distribution for the 45-mm design with thin spacer and solid iron.

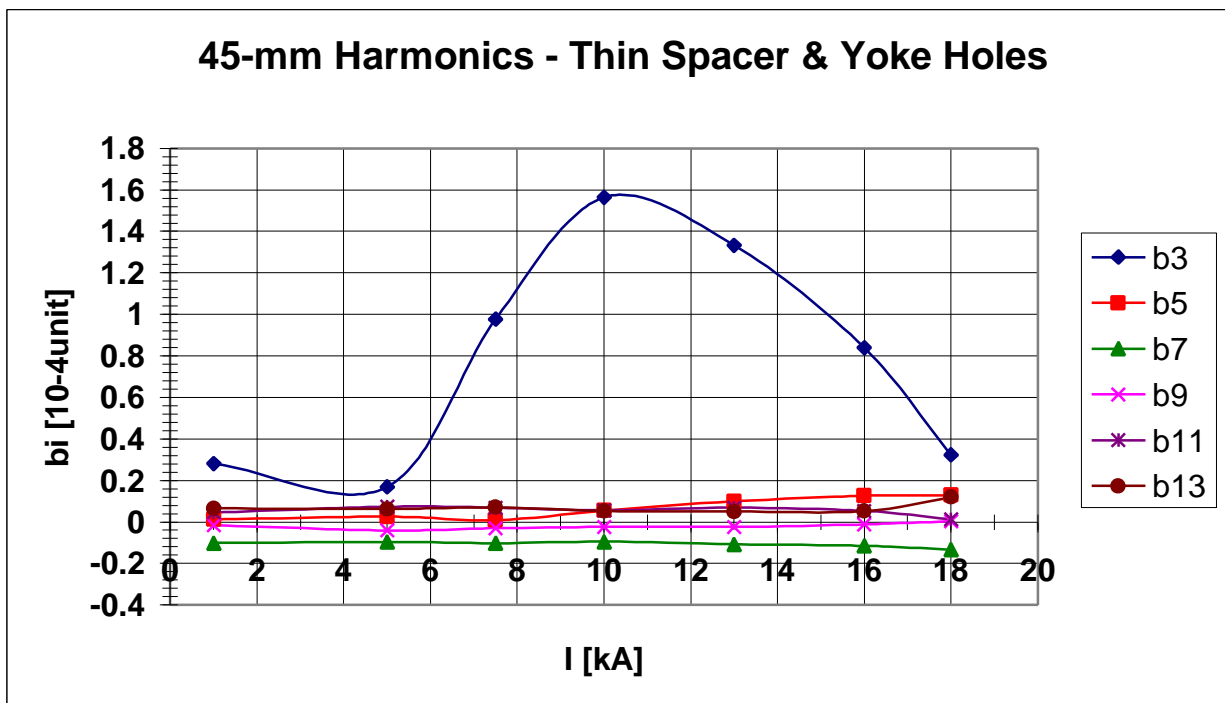


Figure 7b. Harmonics distribution for the 45-mm design with thin spacer and iron yoke holes.

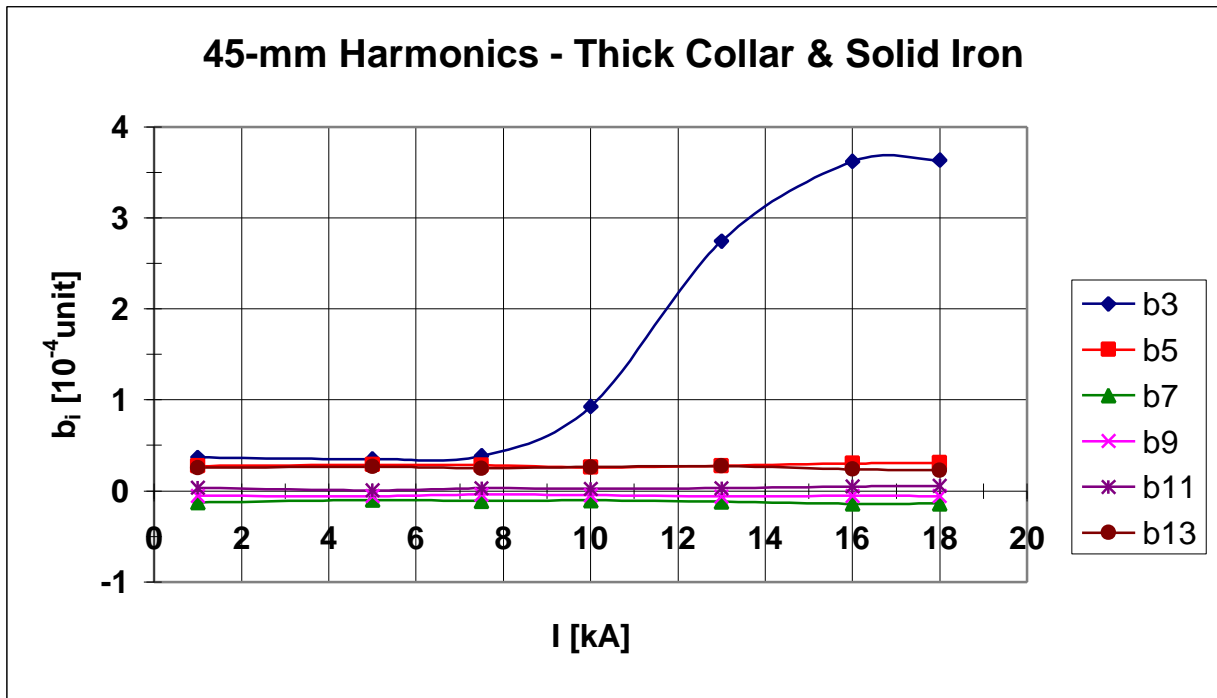


Figure 8a. Harmonics distribution for the 45-mm design with thick collar and solid iron.

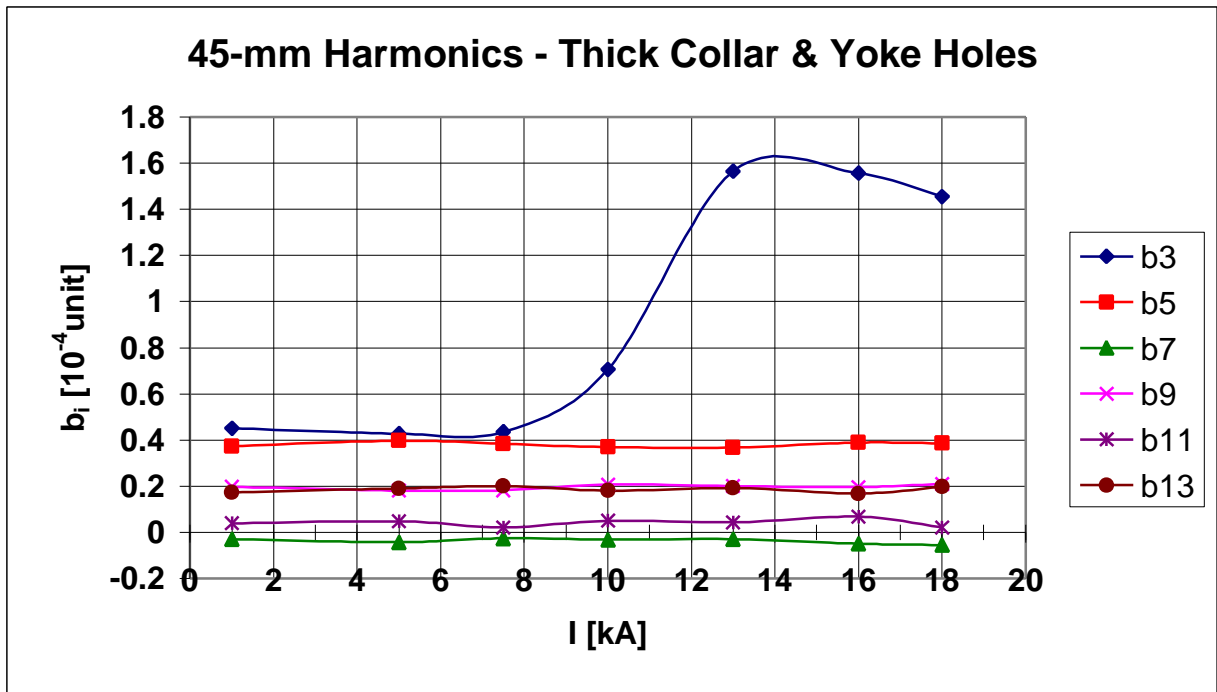


Figure 8b. Harmonics distribution for the 45-mm design with thick collar and iron yoke holes.

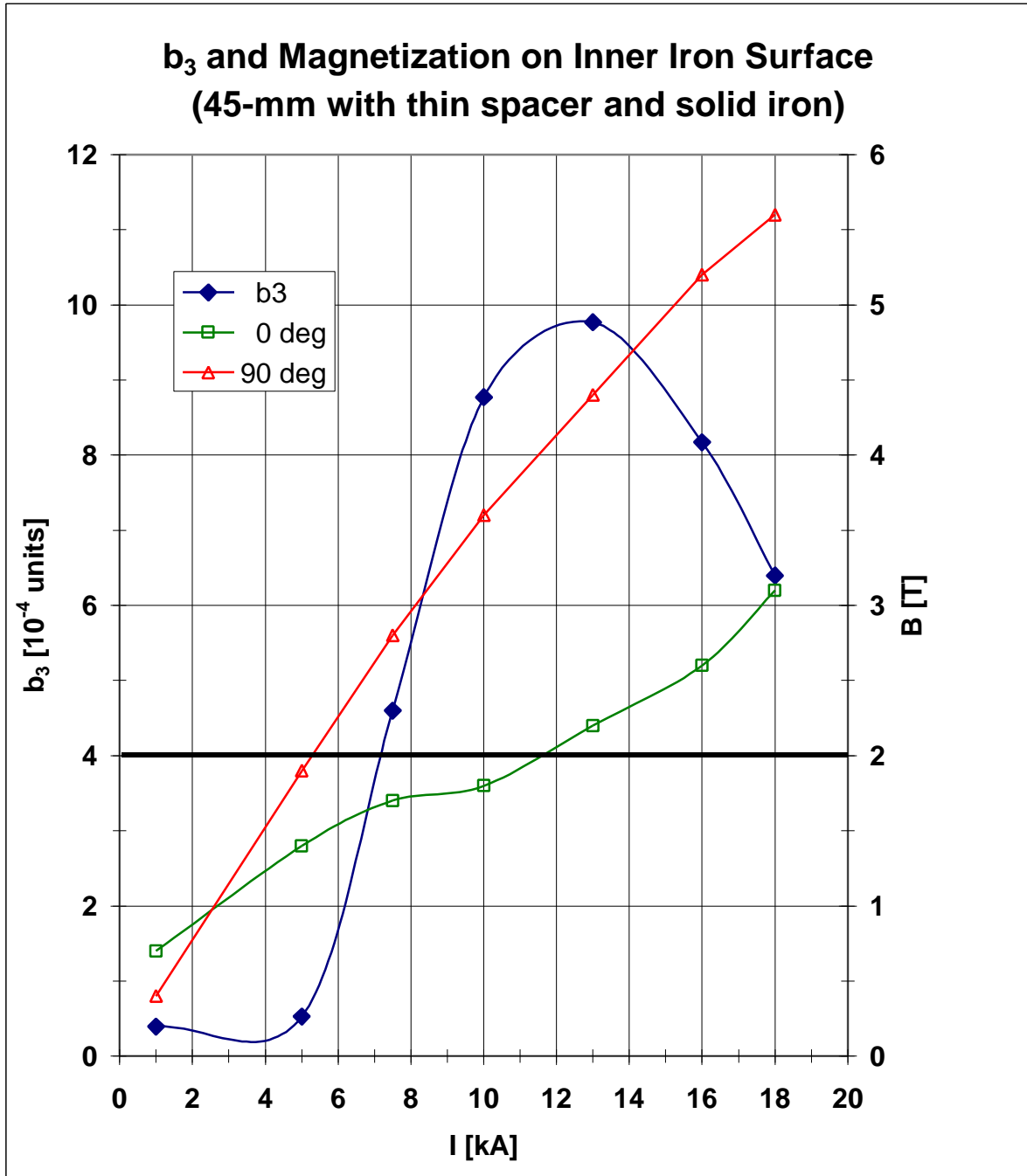


Figure 9. Sextupole variation shown together with excitation curves of inner iron edge at 0° and 90°.

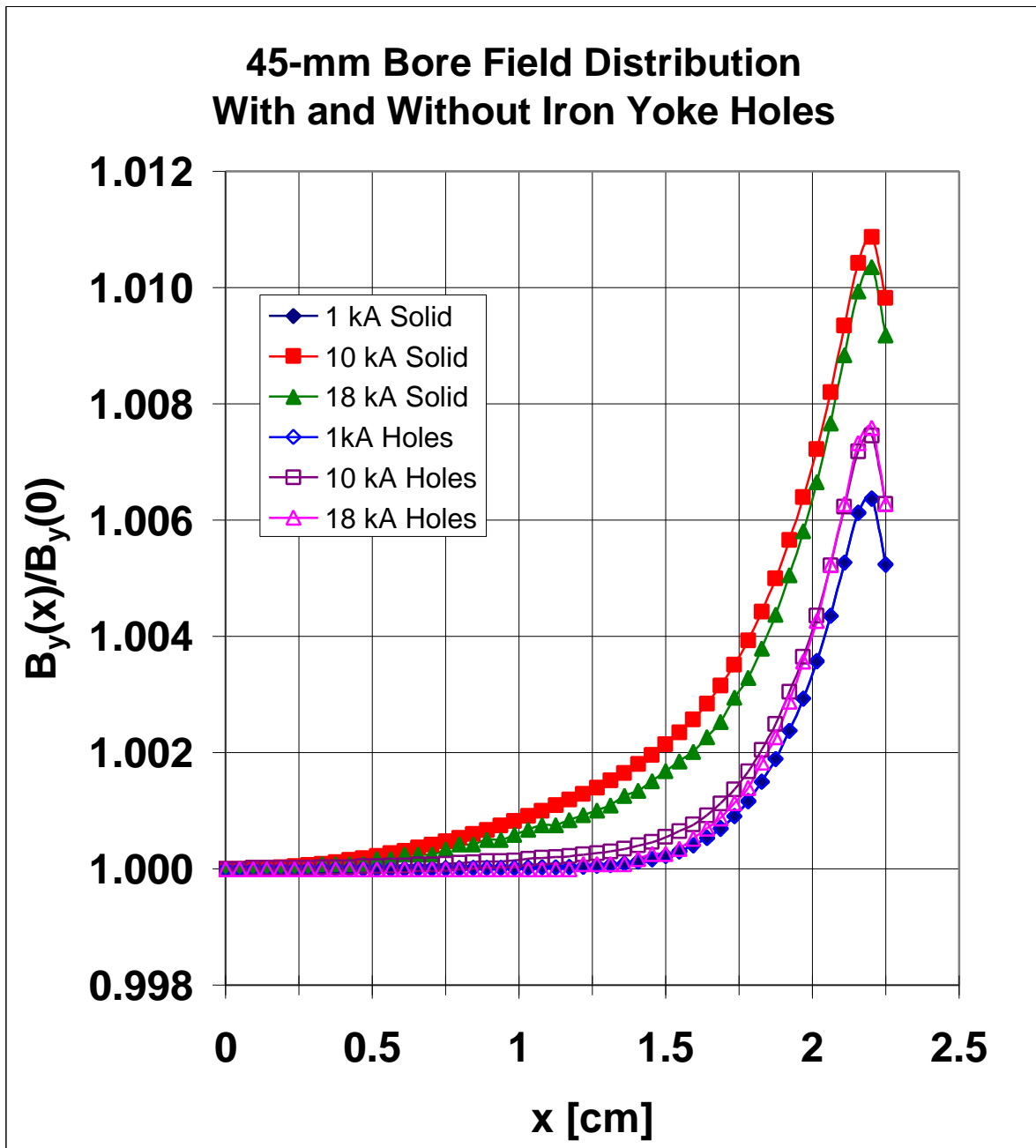


Figure 10. Field distribution $B_y(x)$ on the median plane for the 45-mm thin spacer magnet with and without iron yoke holes.